A New Approach for Describing and Solving the Reversible Briggs-Haldane Mechanism using Immobilized Enzyme

Marco Carrazco-Escalante,[1] José Caro-Corrales,[1,2] Rosalina Iribe-Salazar,[1] Erika Ríos-Iribe,[2] Yessica Vázquez-López,[3] Roberto Gutiérrez-Dorado[1,2] and Oscar Hernández-Calderón[4*]

1. Posgrado en Ciencia y Tecnología de Alimentos, Facultad de Ciencias Químico Biológicas, Universidad Autónoma de Sinaloa, C.P. 80013, Culiacán, Sinaloa, México

2. Programa Regional de Posgrado en Biotecnología, Facultad de Ciencias Químico Biológicas, Universidad Autónoma de Sinaloa, C.P. 80013, Culiacán, Sinaloa, México

3. Posgrado en Ciencias Agropecuarias, Facultad de Medicina, Veterinaria y Zootecnia, Universidad Autónoma de Sinaloa, C.P. 80260, Culiacán, Sinaloa, México

4. Departamento de Ingeniería Química, Facultad de Ciencias Químico Biológicas, Universidad Autónoma de Sinaloa, C.P. 80013, Culiacán, Sinaloa, México

Recently immobilized enzymes have been widely used in industrial processes due to their outstanding advantages, such as high stability and recyclability; however, their kinetic behaviour is generally controlled by mass diffusion effects. Thus, in order to improve these enzymatic processes, a clear discernment between the kinetic and diffusion mechanisms that control the production of the metabolite require investigation. In practice, it is typical to establish apparent kinetics for immobilized enzyme operations, and the validity of the apparent kinetics is restricted to the studied cases. In this work, a new approach for mathematically describing the kinetic and diffusion mechanics in an immobilized biocatalyst bead is established, in which the fraction of residual enzymatic activity is included, and is defined as a measure of the active and available enzymes in the bead porous network. In addition, the diffusion and kinetic mechanisms are described by the effective diffusion coefficient and the free enzyme kinetics, since the porous network of the bead is assumed as the bioreaction volume. Therefore, free enzyme kinetics were determined from glucose to fructose bioconversion using a stirred tank reactor with free glucose-isomerase, in which substrate and enzyme concentrations and temperature were varied. The fraction of residual enzymatic activity ($\eta = 0.553$) and the effective diffusion coefficient ($D_{eff} = 8.356 \times 10^{-12}$ m^2/s) were obtained from the isomerization of glucose to fructose using a stirred tank reactor with immobilized glucose-isomerase in calcium alginate beads at different substrate and enzyme concentrations. Finally, simulations were carried out to establish the bioreaction solid-phase characteristics that most significantly influence productivity.

Keywords: immobilized enzyme, glucose-isomerase, diffusional effects, residual enzymatic activity, simulation

INTRODUCTION

Enzymes are macromolecules produced by living cells that catalyze physiologically significant reactions.[1] Advances in science have led to a large variety of enzymes being employed in industrial processes, leading to their enhanced use with the substrates of interest. The immobilization of enzymes consists of fixing their protein chains to different supports by using various carrier and coupling techniques, which allow the enzyme to be physically separated from the substrate and product for reuse.[2] The advantages of immobilized-enzyme systems can be summarized as follows: (1) repetitive use of an enzyme batch in different reactors; (2) improved process control, as enzymes can be removed from reactants; (3) better stability since they promote the stabilization of the tertiary structure and anti-turbulence factors; (4) enzyme-free products; (5) long half-lives and predictable decay rates; and (6) adequate for use when studying in vivo kinetics of enzymes.[3,4] In general, the main reason for the use of immobilized enzyme systems is related to the reduction of operating costs, caused by using high-price enzymes or obtaining products with low economic value in large-scale continuous systems. However, the immobilized enzyme process has some disadvantages that require improvement: (1) low load of enzymes; (2) restricted diffusion of substrate to the enzyme; (3) low entrapment efficiency, occurrence of burst release, instability of encapsulated enzyme; and (4) little increase in the substrate affinity constant.[5]

Glucose isomerase (GI) is widely used in the industry to catalyze the reversible conversion of α-D-glucose to β-D-fructose, which is part of the production process of high fructose corn syrup (HFCS) from corn starch.[6] Interestingly, enzymatic glucose isomerization was first accomplished on an industrial scale in 1967, and immobilized GI was marketed under the trade name Sweetzyme® by Novozymes in 1974. Today, the enzyme commands the biggest market in the food industry.[7,8] GI Sweetzyme® is not typically used in a stirred tank reactor (STR) due to its poor resistance to shear stress. On the other hand, the use of GI Sweetzyme® in a fixed bed reactor leads to low

conversion, which is caused by the high resistance to convective mass transfer. In addition, there is a high resistance to diffusive mass transfer in an immobilized biocatalyst bead, which is a result of the material and procedure used in the immobilization process. Therefore, it is essential to search for new materials to improve the mechanical and diffusional characteristics of the immobilization process. Indeed, entrapment in calcium alginate beads (CAB) is one of the most widely used techniques for immobilizing enzymes, due to the high gel strength, low shrinkage, and high permeability of alginates.[9,10] Among the research conducted about using immobilized GI, the following stand out: Camacho-Rubio et al.[11] studied fructose-to-glucose isomerization kinetics using Sweetzyme T® in a packed-bed recirculation reactor; Converti and Del Borghi[12] tested the activity of immobilized glucose isomerase in a batchwise reactor (commercial Sweetzyme T®) in order to gather the related kinetic parameters necessary to optimize an immobilized enzyme continuous column reactor; Bravo et al.[13] studied the fructose-glucose enzymatic isomerization using immobilized Sweetzyme A®, considering the effects of internal and external transport; Tükel and Alagöz[14] reported the kinetics of immobilized GI in Eupergit C 250 L in order to determine the activities of immobilized GI using classical Michaelis-Menten kinetics; Abdel-Rassol et al.[6] established a reactor model, which is analogous to heterogeneous catalytic reactor models, taking into account the effects of fluid/particle mass transfer and intraparticle transport; Zhao et al.[15] enhanced the glucose isomerase activity by immobilizing silica/chitosan hybrid microspheres; and Jia et al.[16] described an immobilized method using tris (hydroxymethyl) phosphine as a cross-linker to improve the thermostability of recombinant GI.

Modelling and mathematical simulation used to describe kinetic and diffusion mechanisms are valuable tools for bioreactors design and improvement. In general, free enzyme kinetics are represented by elementary reaction mechanisms, and the Michaelis-Menten mechanism can be highlighted among them, which is expressed as follows: $E + s \underset{k_{-1}}{\overset{k_1}{\rightleftharpoons}} ES \overset{k_2}{\rightarrow} E + P$, where the reaction rate is established by $d[P]/dt = V_m[S]/(K_m + [S])$. The kinetic parameters V_m (maximum rate achieved) and K_m (Michaelis-Menten affinity constant) can be written in terms of the specific rate constants ($V_m = k_2[E]$ and $K_m = (k_{-1} + k_2)/k_1$), which obey the Arrhenius law. In practice, it is typical only to determine the V_m and K_m parameters; however, optimization requires a complete understanding of the dependence of the specific rate constants on temperature, since enzymatic activity is strongly affected by this factor. For immobilized enzyme kinetics, it is necessary to evaluate diffusive and convective mass transfer resistances. However, there are many reports in which a free enzyme kinetic model is adjusted to experimental substrate concentrations, measured in the fluid phase of a STR or a packed-bed at high flow rates; thus, convective effects are negligible and diffusional effects are included in the kinetic parameters. These kinetic models are labelled as apparent and their validity is restricted only to the studied cases. Some representative studies that use the apparent kinetic parameters approach are the following: Özdural et al.[17] established a numerical method for calculating the apparent kinetic parameters in packed-bed immobilized enzyme reactors; Silva et al.[18] reported the kinetic parameters of the α-amylase immobilized on glyoxyl agarose for starch hydrolysis; Das

et al.[19] presented a kinetic study of β-glucosidase entrapped in alginate beads for cellobiose hydrolysis, and from the obtained apparent kinetic parameters, determined that these beads did not have internal mass transfer limitations and Rakmai and Cheirsilp[20] performed the enzymatic synthesis of β-cyclodextrin from starch by immobilized CGTase in a continuous STR and a packed-bed reactor and compared both reaction systems using apparent kinetic parameters. Although it is possible to conceptualize substrate concentration in the intraparticle fluid phase, it cannot be experimentally determined. However, it is possible to incorporate this concentration in a mathematical model, in which the porous network is considered as the bioreaction zone. The model is described in terms of the kinetic and mass transfer mechanisms for the solid phase (i.e., the obtained free enzyme kinetics, an appropriate effective diffusion coefficient (EDC)), and the mass balance between the solid and fluid phases. Thus, fluid-phase concentration data can be obtained from this model and used to adjust the EDC by comparing it to the experimental data. However, there is one drawback; the active and available enzyme concentration in the intraparticle fluid phase is unknown because a few enzyme active sites are usually deactivated or obstructed during the immobilization process. However, this concentration can be included in the mathematical model to obtain a more accurate description of the process.

This study aims to apply a new approach for modelling the phenomenological behaviour of a STR using immobilized enzyme beads. The case study selected for this work is the bioconversion of glucose to fructose using immobilized GI in CAB. First, free-enzyme kinetics data were obtained from a STR using free GI, in which substrate and enzyme concentrations varied, as did the temperature. The reversible Briggs-Haldane mechanism was used for describing the experimental obtained data. The Arrhenius parameters related to the reaction rate constants of the mechanism were simultaneously optimized by a non-linear least-squares method using the Gauss-Newton algorithm with Jacobian and Hessian matrices in explicit form. Subsequently, the bioconversion of glucose to fructose was carried out in an STR using immobilized GI in CAB at different substrate and enzyme concentrations. A novel mathematical model was developed that considered the diffusional and kinetic mechanisms inside a bead, in which the bioreaction zone is the bead porous network, and the mathematical model is described in terms of the free enzyme kinetics, the fraction of residual enzymatic activity (FREA), and the bead EDC. This mathematical model was discretized by the orthogonal collocation method using Hermite cubic splines (OCM-HCS). The resulting ordinary differential equations system was integrated by the Dormand and Prince method,[21] and the model parameters were optimized using the simplex search method.[22] Finally, simulations were carried out to establish the bioreaction solid-phase characteristics that most significantly influence productivity.

MATHEMATICAL MODELS

Free Enzyme Kinetics

The enzymatic isomerization of α-D-glucose to β-D-fructose is represented by the following equation:

$$\alpha - D - \text{glucose} \underset{\text{isomerase}}{\overset{\alpha\text{-glucose}}{\rightleftharpoons}} \beta - D - \text{fructose} \tag{1}$$
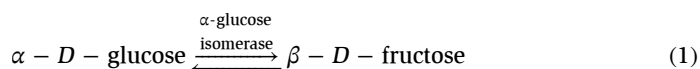
This is a reversible reaction, which can be described by the Briggs-Haldane mechanism:

$$S + E \underset{k_{-1}}{\overset{k_1}{\rightleftharpoons}} X \underset{k_{-2}}{\overset{k_2}{\rightleftharpoons}} P + E \tag{2}$$

Applying the quasi-stationary method, it is possible to obtain a general expression for substrate consumption $(- \mathbf{r}_1)$ and product generation $(\mathbf{r}_2)$ reaction rates, in terms of substrate and product (c_1 and c_2) concentrations, this can be seen as follows:

$$- \mathbf{r}_1 = \mathbf{r}_2 = \frac{\frac{V_{mf}}{K_{mf}}c_1 - \frac{V_{mr}}{K_{mr}}c_2}{1 + \frac{c_1}{K_{mf}} + \frac{c_2}{K_{mr}}} \tag{3}$$

where the kinetic parameters V_{mf} and K_{mf} correspond to the maximum reaction rate and the Michaelis-Menten affinity constant for the conversion of substrate to product, respectively, while V_{mr} and K_{mr} are the analogous parameters for the reverse reaction. These parameters can be obtained from the elementary reaction rates (k_1, k_2, k_{-1}, and k_{-2}) and total enzyme concentration $[E]$ by the following expressions:

$$V_{mf} = k_2[E]; \quad K_{mf} = \frac{k_{-1} + k_2}{k_1}; \quad V_{mr} = k_{-1}[E];$$

$$K_{mr} = \frac{k_{-1} + k_2}{k_{-2}}; \quad K_{eq} = \frac{V_{mf}K_{mr}}{V_{mr}K_{mf}} \tag{4}$$

where K_{eq} is the equilibrium constant of the reaction,[11,13,23,24] and the reaction rate constants are given as follows:

$$k_m = A_m \exp\left(-\frac{E_{a,m}}{RT}\right) \quad m = 1, 2, -1, -2 \tag{5}$$

Immobilized Enzyme Kinetics

The methodology applied to describe the kinetic behaviour in mathematical terms is one of the main problems in the study of immobilized enzyme reactor systems (IERS). This is because the experimental data of substrate and product concentrations obtained in the fluid phase of a bioreaction are directly adjusted with the kinetic mechanism of free enzyme. In this way, apparent kinetic parameters are obtained, which are only valid for the reported conditions. Therefore, the limitations associated with the diffusive mass transfer are unknown and any variation in geometry of the immobilizing matrix is impossible to predict. Furthermore, in these biocatalytic systems, it is difficult to establish the enzyme concentration that was used, since there are different reference volumes (total volume of bioreaction, bead volume, or volume of intraparticle fluid). There are also more complex aspects to consider such as the FREA evaluation after subjecting the enzyme to an immobilization process. Therefore, it is of utmost importance that mathematical description enables the clear discernment of the effect of the factors that have a significant influence on the reaction and mass transport mechanisms, and, thus, to quantitatively establish the importance of these factors in bioconversion productivity.

The mass transfer of a chemical species i in a biocatalytic bead can be expressed through the following differential equation:[25,26]

$$\varepsilon_p \frac{\partial c_i}{\partial t} = D_{eff,i}\left(\frac{\partial^2 c_i}{\partial r^2} + \frac{2}{r}\frac{\partial c_i}{\partial r}\right) + \varepsilon_p \hat{\mathbf{r}}_i \tag{6}$$

The initial and boundary conditions are the following:

$$t > 0, \quad r = 0, \quad \frac{\partial c_i}{\partial r} = 0; \quad t > 0, \quad r = r_p, \quad -D_{eff,i}\frac{\partial c_i}{\partial r}$$

$$= k_{L,i}(c_i - C_i); \quad t = 0, \quad 0 \le r \le r_p, \quad c_i = c_{i,0} \tag{7}$$

where $\hat{\mathbf{r}}_i$ is the volumetric reaction rate based on total volume of bead pores; $D_{eff,i}$ is the EDC inside the particle; ε_p is the biocatalytic bead porosity; C_i is the liquid phase concentration; $k_{L,i}$ is the convective mass transfer coefficient of the fluid phase; and r_p is the biocatalytic bead radius. In this case, the subscript i denotes the chemical species: glucose ($i = 1$) and fructose ($i = 2$), while the subscript 0 represents an initial condition. On the other hand, $\hat{\mathbf{r}}_i$ can be defined from the free enzyme reaction rate ($\mathbf{r}_i$), the latter being obtained through kinetic tests in a free enzyme reaction system (FERS). The dimensional units of $\mathbf{r}_i$ are defined by $V_{mf} = k_2[E]$, where enzyme concentration is given by $[E] = m_{E,t}/V_t$, which is the ratio of the total enzyme mass ($m_{E,t}$) to total reaction volume (V_t, liquid phase). In an IERS, the enzyme is only located inside the beads. In fact, considering that only a fraction of the enzyme is active and available in the liquid phase (pores) of the bead after the immobilization process, the effective enzyme concentration (EEC) in the bead pores can roughly be estimated as $[E]_{imm} = \eta m_{E,t}/(\varepsilon_p V_{p,t})$, and η, $m_{E,t}$, and $V_{p,t}$, are the fraction of residual enzymatic activity, the total immobilized enzyme mass, and the total beads volume, respectively. Using the total volume of reaction (V_t) as a reference, EEC can be expressed as $[E]_{imm} = \eta m_{E,t}/[\varepsilon_p(1 - \varepsilon)V_t]$, where ε is the volumetric fraction of liquid phase in the reaction system. Therefore, for an IERS that uses the same ratio of total enzyme to reaction volume ($m_{E,t}/V_t$) as a FERS, the following relationship is fulfilled:

$$\frac{[E]_{imm}}{[E]} = \frac{\eta}{(1 - \varepsilon)\varepsilon_p} \tag{8}$$

The IERSs have higher concentrations of enzyme mass/reaction volume than the FERS. In general, establishing the design of a reactor based on the relationship $m_{E,t}/V_t$ is a very simple task, regardless of the reactor or bead geometries, based on knowledge of the bead synthesis process. Thus, it is possible to establish that for an IERS that complies with the ratio, $m_{E,t}/V_t$, the reaction rate is given as follows:

$$- \hat{\mathbf{r}}_1 = \hat{\mathbf{r}}_2 = \frac{\frac{\eta}{(1-\varepsilon)\varepsilon_p}V_{mf}\left(c_1 - \frac{c_2}{K_{eq}}\right)}{K_{mf} + c_1 + \frac{K_{mf}}{K_{mr}}c_2} \tag{9}$$

Note that V_{mf} corresponds to that obtained in a FERS, using $m_{E,t}/V_t$. Hence, it is possible to express the reaction rate in a bead ($\hat{\mathbf{r}}_i$) in terms of the obtained free enzyme reaction rate ($\mathbf{r}_i$), which turns out to be a more practical representation for analysis and design purposes, and this can be seen as follows:
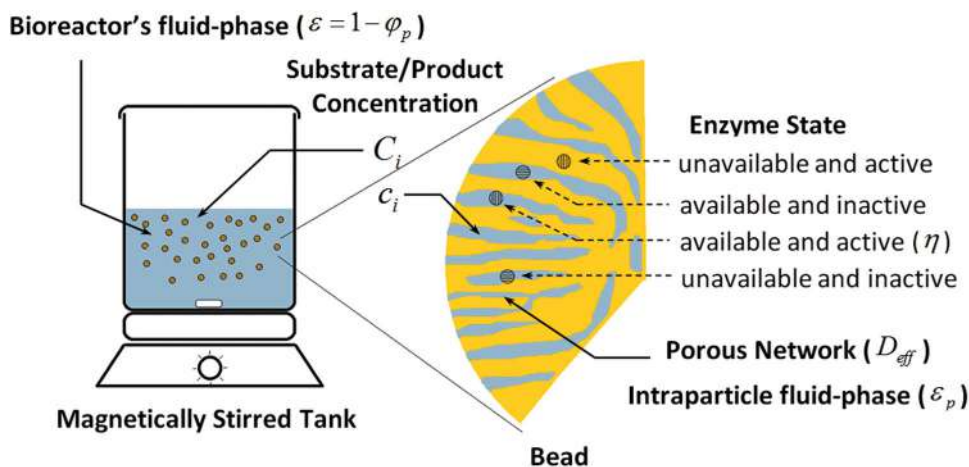
Figure 1. Phenomenological description used in the mathematical model.

$$\hat{r}_i = \frac{\eta}{(1 - \varepsilon)\varepsilon_p}\mathbf{r}_i \tag{10}$$

Naturally, the establishment of the reaction rate expressed by Equation (10) requires the evaluation of the η factor, which is a measure of the immobilization process biocatalytic efficiency with regard to the reaction rate. This is because during the immobilization process a mass fraction of enzyme is affected by the process itself and by the selected immobilization agent during the synthesis of biocatalytic beads. Particularly, the immobilizing agent deactivates and/or blocks a number of active sites from the total immobilized enzyme, thus reducing its biocatalytic capacity (Figure 1).

The dimensional units of $\hat{r}_i$ (from the definition of $[E]_{imm}$) correspond to the volumetric reaction rate based on the volume of bead pores. Regarding the FREA (η), for its experimental evaluation, it is necessary to eliminate the effect exerted by the convective mass transfer over the bioconversion process, which is possible to achieve through kinetic assays of free and immobilized enzymes in an STR under a high hydrodynamic regime. From kinetic assays of free enzyme, the kinetic expression of $\mathbf{r}_i$ can be determined; and from kinetic assays of immobilized enzyme, the FREA (η) is evaluated through the following differential equations system whose solution is adjusted to the obtained experimental data:

$$\varepsilon_p\frac{\partial c_i}{\partial t} = D_{eff,i}\left(\frac{\partial^2 c_i}{\partial r^2} + \frac{2}{r}\frac{\partial c_i}{\partial r}\right) + \frac{\eta}{1 - \varepsilon}\mathbf{r}_i \tag{11}$$

$$V_\infty\frac{dC_i}{dt} = -V_p\hat{a}_pD_{eff,i}\frac{\partial c_i}{\partial r}\bigg|_{r=r_p} \tag{12}$$

The initial and boundary conditions are the following:

$$r = 0, \quad t > 0, \quad \frac{\partial c_i}{\partial r} = 0; \quad r = r_p, \quad t > 0,$$
$$c_i = C_i; \quad 0 \leq r \leq r_p, \quad t = 0, \quad c_i = c_{i,0}; \quad t = 0, \quad C_i = C_{i,0} \tag{13}$$

where $\mathbf{r}_i$ is given by the free enzyme reaction kinetics expressed in Equations (3) and (4), that complies with the ratio $[E] = m_{E,t}/V_t$,

which is also equal to the ratio of the total mass of beads to the total reaction volume of IERS in a STR. Furthermore, V_∞ and V_p are the volume of the liquid (supernatant) and solid (bead) phases of the bioreactor, which in terms of the volumetric fraction of the particle ($\varphi_p = V_p/(V_\infty + V_p)$), Equation (12) can be rewritten as follows:

$$\frac{dC_i}{dt} = -\frac{\varphi_p}{1 - \varphi_p}\hat{a}_pD_{eff,i}\frac{\partial c_i}{\partial r}\bigg|_{r=r_p} \tag{14}$$

where $\hat{a}_p$ is the specific particle area (for a spherical particle of radius r_p, $\hat{a}_p = 3/r_p$).

MATERIALS AND METHODS

Experimental

Materials

Immobilized glucose isomerase (IGI), Sweetzyme IT® was used, produced from a *Streptomyces murinus* strain and distributed by Novozymes (Denmark). IGI particles were immobilized on a glutaraldehyde-based support, which had a cylindrical shape, with a ~0.6–0.8 mm diameter and a 1.4–1.8 mm length. The specific dry activity of IGI, according to the manufacturer, is higher than 5.83 pkat/kg (350 U/g). Glucose ($C_6H_{12}O_6$), magnesium sulphate heptahydrate ($MgSO_4 \cdot 7H_2O$), sodium sulphite (Na_2SO_3), sulphuric acid (H_2SO_4), sodium alginate ($C_6H_7O_6Na$), and calcium chloride ($CaCl_2$) were obtained from Sigma-Aldrich.

Analysis method

A refractometer + polarimeter (ATAGO, RePo-2, Japan) was used to measure glucose and fructose concentrations. The determination is based on associating the concentration in °Brix of the sample with the rotation angle, which is specific for each of these sugars.

Experimental apparatus

All experiments were performed in a 500 mL jacketed STR. The heating system (Thermo Precision, 51221081, USA) was able to adjust the reactor temperature to an accuracy of ±1 °C. Hot

water was used to maintain the reactor temperature. The reactor was sealed with aluminum foil during the experiments to prevent loss of water by evaporation. To decrease the convective effects, a magnetic stirrer heating plate (Barnstead, SP131015, USA) was used and the rotation speed was adjusted to 880 rpm ($D_{st} = 0.029$ m, $D_{ir} = 0.073$ m, $h_L = 0.060$ m).

Experimental procedures

For free enzyme kinetics, a mortar and pestle were used for the pulverization of enzyme prior to each experimental run. The dimensions of the enzyme particles were reduced as much as possible and their size was determined by a stereomicroscope (Motic, DM143, China), obtaining an approximate size from 60−90 μm in diameter, which was considered as free enzyme. To choose the optimal working temperature, several tests were carried out at different temperatures (55, 60, 65, and 70 °C), with a constant substrate concentration of 100 g/L (0.556 mol/L) and enzyme concentration of 5 g/L. The bioconversion of both glucose to fructose and fructose to glucose was studied. Once the optimum temperature was determined, different initial glucose concentrations of 100 g/L (0.556 mol/L), 150 g/L (0.833 mol/L), and 200 g/L (1.111 mol/L), and catalyst loading (5, 7.5, and 10 g/L) were tested. All experiments were carried out at a constant pH (7.5) for a 210 min period. The initial glucose solution (250 mL) was prepared as reported by Dehkordi et al.[24] by dissolving the required amount of glucose in deionized water and then adding 0.7 g of $MgSO_4 \cdot 7H_2O$ and 0.7 g of Na_2SO_3 in order to stabilize the enzyme and eliminate dissolved oxygen, respectively. The pH was adjusted to 7.5 with H_2SO_4 1N. In each experiment, the feed solution with the desired volume, concentration, temperature, and pH was fed to the reactor. Then, the rotation speed was adjusted to 880 rpm and the reactor temperature was maintained at the desired value. Later, the required amount of catalyst was suddenly added to the reactor. This instant was considered as the start time of the reaction. During the course of the reaction, samples were taken at 5, 10, 20, 30, 40, 50, 60, 80, 100, 120, 150, 180, and 210 min. The progress of the reaction inside the samples was stopped by the addition of H_2SO_4 1N. The analysis of the samples was performed by the aforementioned method for glucose-fructose concentrations.

In order to evaluate the diffusional effects on the conversion of glucose to fructose, a STR system similar to that previously described was used; however, in this case the free enzyme was immobilized in CAB. For that matter, the Tumturk et al.[10] methodology was used with some modifications. A system consisting of a funnel, a needle valve, and a pipette tip of 1 mL was mounted on a universal support and they were connected to each other by small pieces of latex hose. The desired amount of free enzyme (1.25, 1.875, or 2.5 g) was added to a solution of sodium alginate (175 mL, 2 % w/v). Then, 7.0 mL of glutaraldehyde solution (5.0 %) was added as a bifunctional reagent, in order to improve the stability of the gel beads. This solution was gently stirred and dropped into a $CaCl_2$ (0.3 mol/L) solution. The resulting spherical CAB were removed and maintained in a diluted solution of $CaCl_2$ (0.03 mol/L) for 1 day at 4 °C. Afterwards, the CAB were washed with deionized water and stored at 4 °C for later use. The size of the beads (3 mm diameter) was controlled by opening or closing the valve. The diameter of the beads was measured using a calliper. Once the enzyme was immobilized and ready for use, the initial conditions of temperature (65 °C), pH (7.5), rotation speed (880 rpm), enzyme concentration (3.213, 4.784, and 6.292 g/L), and substrate concentration (0.556, 0.833, and 1.111 mol/L) were established. The start of the reaction is considered by adding CAB to the reactor, and samples were taken every 30 min for a total period of 210 min.

Method of Adjustment used for the Free Enzyme Kinetic Model

A key aspect in free enzyme processes is the search for kinetic mechanisms whose mathematical representation can describe the experimental data obtained in laboratory. In the case of complex reaction mechanisms, the optimization of the kinetic parameters is usually performed by minimizing the error between the experimental and numerical data. In addition, in each iteration of this numerical technique, it is necessary to obtain the solution of the differential equations system for the studied reaction mechanism. In some kinetic mechanisms under restricted operating conditions, as with Michaelis-Menten kinetics under batch and isothermal bioreaction conditions, it is possible that the kinetic parameters (the maximum reaction rate and the affinity constant for the substrate) can be obtained through the Hanes-Woolf diagram. However, if it is desired to determine the effect of temperature on the kinetic mechanism, it is necessary to evaluate these kinetic parameters at different temperatures. The purpose is to establish the dependency of these kinetic parameters on temperature in terms of the specific rate constants of the kinetic mechanism, which generally obeys the Arrhenius law. In the case of the Briggs-Haldane reversible mechanism, at each time step the substrate/product ratio determines the effect that the kinetic parameters have on the bioreaction kinetic behaviour. Therefore, the individual adjustment of the kinetic parameters from the experimental data will only be accurate in the direction of the reaction, for that studied experiment. In this sense, if the numerical process to adjust the parameters consists first in adjusting the specific rate constants at each constant temperature, and subsequently adjusting the Arrhenius parameters from the obtained specific rate constants, then the best global adjustment of parameters may not be guaranteed. Accordingly, it is essential to establish a numerical methodology that allows the simultaneous adjustment of different kinetics in which bioconversion is considered in both reaction directions at different temperature conditions.

Linearization strategy

In the case of isothermal FERS, it is possible to obtain a linearized solution for Equation (3), in terms of the initial substrate and enzyme concentrations. While the initial substrate and product concentrations are $c_{1,0}$ and $c_{2,0}$, respectively, at equilibrium, it will be true that $c_{1,0} + c_{2,0} = c_{1,eq} + c_{2,eq} = c_0$ (conservation of matter) and $K_{eq} = c_{2,eq}/c_{1,eq}$ (thermodynamic equilibrium), and this can lead to the following equation:

$$c_{2,eq} = \frac{K_{eq}c_0}{K_{eq} + 1} \tag{15}$$

On the other hand, at any time, it is true that $c_1 + c_2 = (K_{eq} + 1)c_{2,eq}/K_{eq} = c_0$, and, hence, Equation (3) can be established in function of the product concentration only. From the definitions set forth in Equation (4), it is possible to integrate Equation (3) and obtain the following expression:

$$t = B_1 \frac{c_2 - c_{2,0}}{[E]} - (B_{21} + B_{22}c_0)\frac{c_2 - c_{2,0}}{[E]\Delta c_{2,m}} \tag{16}$$

where the B_1, B_{21}, and B_{22} coefficients are defined as follows:

$$B_1 = \frac{K_{eq}}{K_{eq}+1}\frac{1}{\bar{V}_{mf}}\left(1 - \frac{K_{mf}}{K_{mr}}\right); \quad B_{21} = \frac{K_{eq}}{K_{eq}+1}\frac{K_{mf}}{\bar{V}_{mf}};$$

$$B_{22} = \frac{K_{eq}}{\left(K_{eq}+1\right)^2}\left(\frac{1}{\bar{V}_{mf}} + \frac{1}{\bar{V}_{mr}}\right) \tag{17}$$

Here, $\bar{V}_{mf} = V_{mf}/[E] = k_2$ and $\bar{V}_{mr} = V_{mr}/[E] = k_{-1}$, therefore, the B_1, B_{21}, and B_{22} coefficients depend on temperature only. Note that Equation (16) is a linearized expression of time with respect to the product concentrations, in which, $\Delta c_{2,m}$ is the logarithmic mean of the differences in final and initial concentrations with respect to the concentration at equilibrium and is defined by the following equation:

$$\Delta c_{2,m} = \frac{c_2 - c_{2,0}}{\ln\frac{c_2 - c_{2,eq}}{c_{2,0} - c_{2,eq}}} \tag{18}$$

After multiplying Equation (16) by the $(c_2 - c_{2,eq})/[t(c_{2,0} - c_{2,eq})]$ factor, it is possible to rewrite Equation (16) in such a way that allows the unaccomplished product ratio to be estimated with respect to the equilibrium conditions (θ):

$$\theta = \alpha B_1 + \beta B_{21} + \gamma B_{22} \tag{19}$$

These parameters are defined by the following expressions:

$$\theta = \frac{c_2 - c_{2,eq}}{c_{2,0} - c_{2,eq}}; \quad \alpha = \frac{(c_2 - c_{2,0})(c_2 - c_{2,eq})}{[E]t(c_{2,0} - c_{2,eq})}; \quad \beta = -\frac{\alpha}{\Delta c_{2,m}};$$

$$\gamma = -\frac{\alpha c_0}{\Delta c_{2,m}} \tag{20}$$

To evaluate the α, β, and γ parameters, it is necessary to provide diverse information, such as the enzyme concentration ([E]), the initial substrate and product concentrations ($c_{1,0}$ and $c_{2,0}$), the equilibrium constant (K_{eq}), as well as the product concentration (c_2) reached over time (t). The B_1, B_{21}, and B_{22} parameters can be evaluated in terms of three specific reaction rates and the equilibrium constant by the following:

$$B_1 = \frac{1}{K_{eq}+1}\left(\frac{K_{eq}}{k_2} - \frac{1}{k_{-1}}\right); \quad B_{21} = \frac{K_{eq}}{K_{eq}+1}\left(\frac{k_{-1}}{k_1 k_2} + \frac{1}{k_1}\right);$$

$$B_{22} = \frac{K_{eq}}{\left(K_{eq}+1\right)^2}\left(\frac{1}{k_2} + \frac{1}{k_{-1}}\right) \tag{21}$$

Here, the equilibrium constant is known a priori and k_1, k_2, and k_{-1} are functions of temperature and the Arrhenius parameters, pre-exponential factor (A_m) and activation energy ($E_{a,m}$), according to Equation (5).

Numerical method to obtain the kinetic parameters

However, it is feasible to determine the specific reaction rates (k_m) by adjusting the linearized kinetic model (Equation (19)), using experimental data, by multiple linear regression; the experimental error, altogether with the kinetic data close to equilibrium, hinder the subsequent numerical process of adjustment for the

Arrhenius parameters (A_m and $E_{a,m}$). This is because there are several adjustment scenarios, in which deviations between experimental and numerical data are similar, even though they are obtained with very different values of A_m and $E_{a,m}$. In this sense, due to the relative simplicity of the linearized kinetic model (Equation (19)), it is possible to apply the multivariate Gauss-Newton algorithm to determine the Arrhenius parameters, allowing the simultaneous adjustment of different isothermal kinetics regardless of the used reaction direction or operating temperature. The model adjustment was proposed by minimizing the sum of squares of errors between the unaccomplished product ratio with respect to the equilibrium condition (θ). Considering N experimental kinetics with M number of tests performed at different times for each kinetic experiment and looking for a simplistic notation to refer to each test, the j-th assay of the k-th kinetics was denoted by $i = j + (k-1)M$. Thus, the method to obtain the Arrhenius kinetic parameters consists of minimizing the following residual sum of squares: SSE $= \sum_{i=1}^{MN} r_i^2$, where $r_i = (\alpha B_1 + \beta B_{21} + \gamma B_{22})_i - \theta_{\exp,i}$. Here, the subscript i indicates that the expression in parentheses is evaluated at the i-th experimental assay conditions. The unknown Arrhenius parameters of the specific reaction rates are represented by a_m and b_m, with $m = 1, -1, 2$, which are shown in the following expression:

$$k_m = a_m^2 \exp\left(-\frac{b_m^2}{RT}\right) \tag{22}$$

Squared unknown parameters were used to avoid assigning negative values during the optimization process. Therefore, in general, if the $\vec{p}$ vector components represent the parameters that minimize the error of the residuals, $\vec{p} = (a_1, b_1, a_2, b_2, a_{-1}, b_{-1})$, these can be obtained by means of the Gauss-Newton method through the following iterative process:

$$\vec{p}_{n+1} = \omega\left\{\vec{p}_n - \left[J_{\vec{r},\vec{p}}(\vec{p}_n)^t J_{\vec{r},\vec{p}}(\vec{p}_n)\right.\right.$$
$$\left.\left. + \sum_{i=1}^{m} r_i(\vec{p}_n)H_{r_i,\vec{p}}(\vec{p}_n)\right]^{-1}J_{\vec{r},\vec{p}}(\vec{p}_n)^t\vec{r}(\vec{p}_n)\right\} + (1-\omega)\vec{p}_n \tag{23}$$

where ω is a sub-relaxation factor ($0 < \omega < 1$); $\vec{r}(\vec{p}_n)$ is the vector of residuals as a function of the vector of adjustment parameters obtained in iteration n; $J_{\vec{r},\vec{p}}$ is the Jacobian of the residual vector $\vec{r}$ with respect to the adjustment parameters $\vec{p}$, that is defined as follows $J_{ij} = \partial r_i/\partial p_j$; and $H_{r_i,\vec{p}}$ is the Hessian of r_i with respect to the $\vec{p}$ adjustment parameters, defined by the following expression $H_{jk} = \partial^2 r_i/\partial p_j \partial p_k$. The explicit forms of Jacobian and Hessian are presented in the Supplementary Material.

Method of Adjustment used for the Immobilized Kinetic Model

Discretization method

One of the fundamental problems to obtain a numerical solution of partial differential equations, such as that expressed in Equation (11), is the applied discretization process in order to obtain the ordinary equations system in each interpolation node. The solution function can vary significantly in a short region of the spatial domain, as a result of the imposed boundary

conditions. This leads to large numerical errors in the obtained solution if an appropriate discretization process is not chosen. Therefore, it is necessary that the implemented numerical methods consider the different behaviours of a family of solutions associated with a differential equations system. Thus, it is expected that for the concentration profiles of a chemical species, in a biocatalytic bead subjected to a high mass transfer resistance, large concentration gradients will be present on the surface of the bead. Therefore, an appropriate discretization procedure for differential equations corresponds to the use of OCM-HCS, because this methodology guarantees the continuity of the solution function as well as its first derivative. The Supplementary Material provides a more detailed description of OCM-HCS.

Numerical method to obtain the adjustment parameters

The mathematical model, expressed by Equations (11) and (14) with their respective boundary and initial conditions (Equation (13)), has the following as unknown parameters: the EDC of the i species inside the particle (D_{eff}) and FREA (η), which were adjusted by the simplex search method of Lagarias et al.[22] Thus, the optimizing method for D_{eff} and η parameters was performed as follows: (1) a variable change was applied for $D_{eff} = a^2$ and $\eta = [\mathrm{erf}(b)]^2$, which guarantees that the search for the D_{eff} value is only in the interval $[0, \infty)$, and for the η value, the search is in the interval $[0, 1]$; (2) the differential equations system expressed by Equations (11), (13), and (14) was coded, in which Equation (11) was previously discretized by OCM-HCS, and this discretized equation describes the diffusive transport and the intraparticle reaction of glucose and fructose; (3) the ordinary differential equations system generated in the previous step, in conjunction with Equation (14), which describes the glucose and fructose balance in the STR liquid phase, was simultaneously integrated by the Dormand and Prince method;[21] (4) the sum of squares of the weighed residuals (SSWR) between the experimental and simulated data was evaluated, and it was used as a criterion for the adjustment of the D_{eff} and η parameters, through the simplex search method.[22] The minimization criterion that was used is as follows: $\mathrm{SSWR} = \sum_{i=1}^{n} \sum_{j=1}^{m} \left(d_{ij}/W_j \right)^2$, where SSWR represents the sum of squares of the weighed residuals, i and j represent the number of experimental data points and the number of variables, respectively, W_j represents the weight of each variable (maximum value of each variable), and d_{ij} denotes the difference between the model and the experimental value.

RESULTS AND DISCUSSION

Free Enzyme Kinetics

Figure 2a shows the experimental data for the conversion of glucose to fructose and fructose to glucose, using only a 0.833 mol/L concentration of glucose or fructose as substrate, respectively, and 5 g/L of free enzyme at different operating temperatures (55, 60, 65, and 70 °C). The selected optimum temperature was 65 °C. Although conversion at 70 °C was slightly higher, the mechanical damage of the beads was much higher compared to 65 °C. The elasticity of calcium alginate decreases with the increase in temperature,[27] favouring the rupture of the beads, and with this, small fractions of beads are dragged into the output of the bioreactor. This damage affects the bead capability for reuse. On the other hand, Figure 2b shows the experimental data for the conversion of glucose to fructose using different initial concentrations of glucose (0.556, 0.833, and 1.111 mol/L), as well as different concentrations of free enzyme (5, 7.5, and
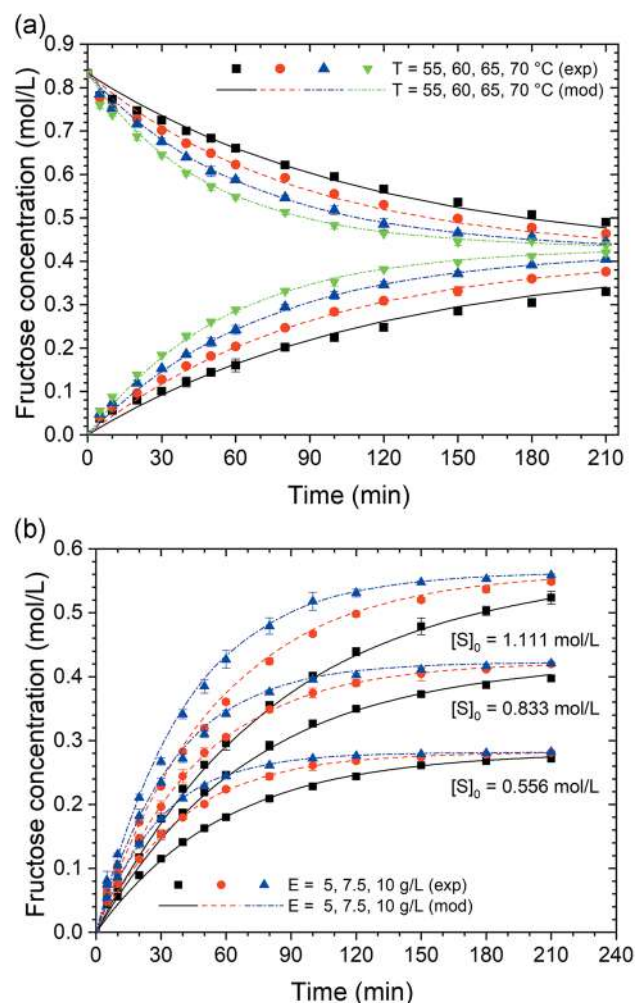
Figure 2. (a) Effect of temperature on the glucose/fructose and fructose/glucose bioconversion kinetics using free enzyme in a STR with 5 g/L of free enzyme and 0.833 mol/L of substrate; and (b) effect of glucose and enzyme concentration on the glucose/fructose bioconversion kinetics using free enzyme in a STR at 65 °C. Bars represent the standard deviation.

10 g/L) at 65 °C. The kinetic model expressed by Equation (3) was simultaneously adjusted to all of the experimental data shown in Figure 2; the obtained results from the adjustment is presented by continuous and semi-continuous lines. An adequate fit between the experimental and simulated data is observed, with a determination coefficient of $R^2 = 0.9974$. The obtained parameters from the adjustment are shown in Table 1.

In addition, Table 2 shows the reversible kinetic parameters of the Briggs-Haldane mechanism given by Equation (2) as well as the experimentally obtained equilibrium constants (55–70 °C, 0.995–1.062) using free enzyme. These constants are in the range (55–65 °C, 0.850–1.170) reported by Dehkordi et al.[24] using immobilized enzyme (Sweetzyme). It can be seen that as temperature increases, the ratio of fructose/glucose concentration also increases. Specifically, the relationship between the maximum rate for fructose production with respect to glucose production (V_{mf}/V_{mr}) decreases, just as the relationship between the Michaelis-Menten affinity constants (K_{mf}/K_{mr}) also decreases. This combination of behaviours causes an antagonism effect in the fructose production, where the ratio of maximum rates

predominates over the affinity constants relationship; this difference is accentuated as temperature increases. Referring to the equilibrium constant, the experimental data were used to adjust the Arrhenius equation parameters, obtaining the following result:

$$K_{eq} = 10.356 \exp\left(-\frac{6489 \text{ J/mol}}{RT}\right) \quad (24)$$

Regarding the numerical methodology implemented to obtain the adjustment of the Arrhenius kinetic parameters, this was carried out in two stages: (1) a first approximation was obtained from the multivariate Gauss-Newton method using the Jacobian of the algebraic nonlinear system only, and (2) this solution was refined by incorporating the Hessian into the numerical methodology. Although it was not included in this work, the Levenberg-Marquardt algorithm was also used, which allowed an acceptable but unbalanced parameter adjustment to be obtained, and the unbalance was due to the kinetics of conversion from glucose to fructose was favoured.

Immobilized Enzyme Kinetics

For the experimental work of bioconversion from glucose to fructose using immobilized enzyme in a STR, the convective mass transfer coefficient was considered negligible, due to the used agitation regime. In addition, the same EDC for glucose and fructose was considered, due to the great similarity between the chemical species. The operating parameters employed in the determination of EDC (D_{eff}) and FREA (η) are listed in Table 3, which were experimentally evaluated. The glucose and fructose concentrations inside the catalytic bead were considered negligible.

Figure 3 shows the experimental data for the conversion of glucose to fructose, using immobilized enzyme in CAB, in terms of glucose concentration (0.556, 0.833, and 1.111 mol/L) and enzyme concentration (3.213, 4.784, and 6.292 g/L). The latter is established as the ratio of total enzyme/total reaction volume ($m_{E,t}/V_t$), similar to a free enzyme reaction system. The mathematical model (Equations (11), (13), and (14)) was simultaneously adjusted using all the experimental data shown in Figure 3, obtaining a

Table 3. Operation parameters for the adjustment of the kinetics with immobilized enzyme in CAB

Operation Parameter	Value		
r_p (m)	1.5×10^{-3}		
T (°C)	65		
ε_p (L/L)	0.919		
$[E]_t$ (g/L)	3.213	4.784	6.292
φ_p (L/L)	0.363		
$C_{1,0}$ (mol/L)	0.556	0.833	1.111
$C_{2,0}$ (mol/L)	0		

satisfactory fit with $R^2 = 0.9910$. The simulated data are shown in Figure 3 by continuous and semi-continuous lines.

The best adjustment gave the following parameters: $D_{eff} = 8.356 \times 10^{-12}$ m^2/s and $\eta = 0.553$. Interestingly, these parameters are adequate for all three different concentrations of enzyme, which suggests that the immobilizing support (calcium alginate matrix) is mainly responsible for establishing the phenomenological behaviour of the EDC and the FREA. In previous works regarding the diffusion of glucose in calcium alginate gel, the reported EDC has been 6.230×10^{-10} m^2/s,[28] 8.350×10^{-10} m^2/s,[29] and 4.974×10^{-11} m^2/s.[26] In this work, the EDC was smaller, indicating a greater restriction to the substrate movement inside the CAB. It is necessary to search for better immobilization conditions that enable better EDCs to be obtained and, therefore, a greater interaction between the substrate and enzyme.

Additionally, the conventional mathematical model (i.e., the kinetic model of free enzyme) was applied on the experimental data of the immobilized enzyme in order to obtain the apparent kinetic parameters. In all of the studied cases, the adjustment was very poor because the diffusional mass transfer resistance is significant. To obtain the apparent kinetic parameters, Equation (16) was rearranged to the following linearized form:

$$\frac{t[E]}{c_2 - c_{2,0}} = B_1 + (B_{21} + B_{22}c_0)\left(-\frac{1}{\Delta c_{2,m}}\right) \quad (25)$$

Thus, according to this mathematical expression, for experimental kinetics with the same concentration of enzyme and at the same operating temperature, it is expected that these kinetics, in their linearized form, had the same intercept (B_1), and a linear slope ($B_{21} + B_{22}c_0$) with respect to the initial total concentration of substrate and product (in this case, $c_0 = c_{1,0}$). In Figure 4, the this is shown in detail.

On the other hand, Figure 5 shows the behaviour of the experimental kinetic data obtained under the linearized form of Equation (25). The experimental data do not behave according to the

Table 2. Kinetic parameters of the Briggs-Haldane mechanism
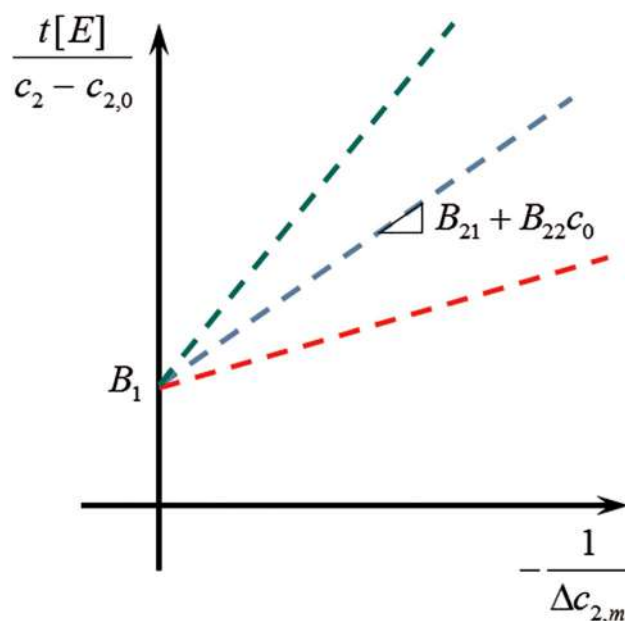
T °C	k_1 L/(mol·s)	k_2 mol/(g·s)	k_{-1} mol/(g·s)	k_{-2} L/(mol·s)	K_{eq}	$\frac{V_{mf}}{V_{mr}}$	$\frac{K_{mf}}{K_{mr}}$
55	5.272×10^{-5}	2.599×10^{-5}	2.859×10^{-5}	4.994×10^{-5}	0.953	0.909	0.947
60	7.735×10^{-5}	3.143×10^{-5}	3.681×10^{-5}	6.639×10^{-5}	1.002	0.854	0.858
65	1.122×10^{-4}	3.779×10^{-5}	4.705×10^{-5}	8.752×10^{-5}	1.030	0.803	0.780
70	1.610×10^{-4}	4.520×10^{-5}	5.971×10^{-5}	1.144×10^{-4}	1.062	0.757	0.711
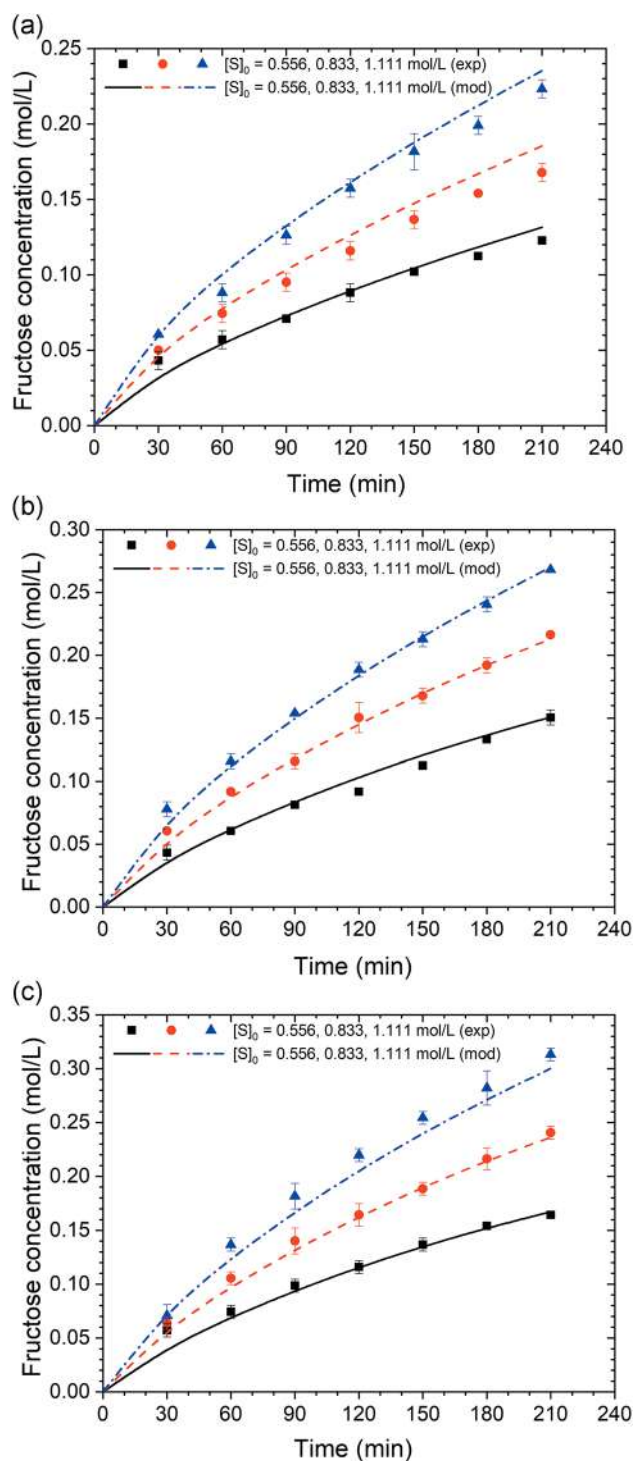
Figure 3. Effect of substrate and enzyme concentration in the bioconversion of glucose to fructose using immobilized enzyme in a STR at 65 °C: (a) 3.213, (b) 4.784, and (c) 6.292 g/L of enzyme. Bars represent the standard deviation.

Figure 4. Effect of the initial concentration on the Briggs-Haldane reversible kinetic mechanism, using the mathematical model of free enzyme in its integrated and linearized form.

kinetic model of free enzyme because they do not have the same value of the intercept for kinetics that only differ in the initial concentration of the substrate. In addition, the kinetics shown in Figures 5a and c (see Table 4) have very similar slopes (parallel straight lines); therefore, any effort to express experimental data through a general model of free enzyme will be unsuccessful. The adjustment para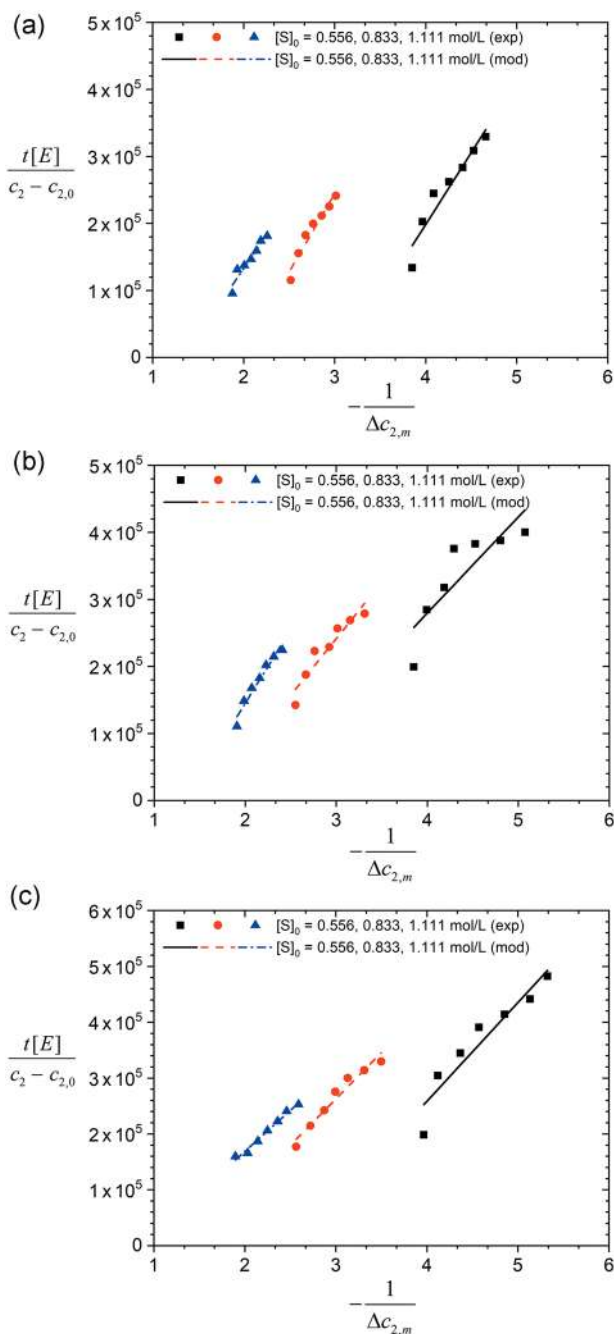meters of the linearized kinetic model of free enzyme are shown in Table 4. For most of the cases, an adequate degree of adjustment for each kinetics was obtained ($R^2 > 0.9$). While each individual kinetics shows a linear behaviour, it is evident that a generalization in the adjustment parameters is not feasible.

Although Dehkordi et al.[24] reported a satisfactory adjustment for the kinetic model of free enzyme obtained from the experimental kinetics of immobilized enzyme in a STR, in this research it was not possible to achieve the same results. Here, the diffusional effects are more significant in the developed experimental assays, making it difficult to obtain a general kinetic model of apparent parameters, even for experimental trials in which only the initial substrate concentration differs. In this sense, these results highlight the strength of the new mathematical modelling approach for the Briggs-Haldane reversible kinetic mechanism using immobilized enzyme in comparison to the use of kinetic models with apparent parameters. It is certainly recognized that the numerical resolution of the model is complex; however, the information that is obtained by adjusting the model is valuable for improving these bioprocesses.

Bidabehere et al.[30] obtained the kinetic, equilibrium, and transport parameters through a pseudo-homogeneous mathematical model. The method was based on assays with two different catalyst particle sizes. For the experimental tests, a well-stirred batch reactor was used, in which a first order chemical reaction was produced and controlled by the diffusion mass transport. It was found that their proposed model appropriately described the obtained experimental data. Although the microscopic balances established for the fluid phase and the catalytic particle are very similar to those reported in this work, the effect of the catalyst concentration inside the porous network of the catalytic support was not studied. Also, this effect was not explicitly established in the mathematical model; instead, only the constant of the reaction rate was determined. Bidabehere et al.[30] concluded that the proposed mathematical model was successful and determined that their methodology was more general than conventional models. Conventional models consider the concentration profiles inside the

Figure 5. Behaviour of experimental kinetic data of immobilized enzyme with respect to the linearized model of free enzyme: (a) 3.213, (b) 4.784, and (c) 6.292 g/L of enzyme.

Table 4. Adjusted parameters of the linearized model of free enzyme used to describe experimental kinetic data of immobilized enzyme

$c_{1,0}$ (mol/L)	[E] (g/L)	B_1 (g · s/mol)	$B_{21} + B_{22}c_0$ (g · s/L)	R^2
0.556	3.213	-6.576×10^5	2.141×10^5	0.9186
0.833		-4.532×10^5	2.324×10^5	0.9445
1.111		-2.708×10^5	2.017×10^5	0.9300
0.556	4.784	-2.938×10^5	1.434×10^5	0.7363
0.833		-2.656×10^5	1.690×10^5	0.8983
1.111		-2.944×10^5	2.197×10^5	0.9525
0.556	6.292	-4.501×10^5	1.771×10^5	0.9009
0.833		-2.361×10^5	1.662×10^5	0.9538
1.111		-1.250×10^5	1.469×10^5	0.9831

not contain an analysis of experimental data to establish the feasibility of the proposed model, nor does it contain the concept of enzymatic efficiency associated to the immobilization process. On the other hand, they use porosity to describe the specificity in the concentration distribution of the substrate between two neighbouring regions: the concentration of the substrate in the MRs; and the concentration in the bulk solution. Additionally, they do not present an analysis of the effects of the design parameters on the intraparticle substrate concentration, as is done in this work. They focus their attention on the evaluation of the effectiveness factor.
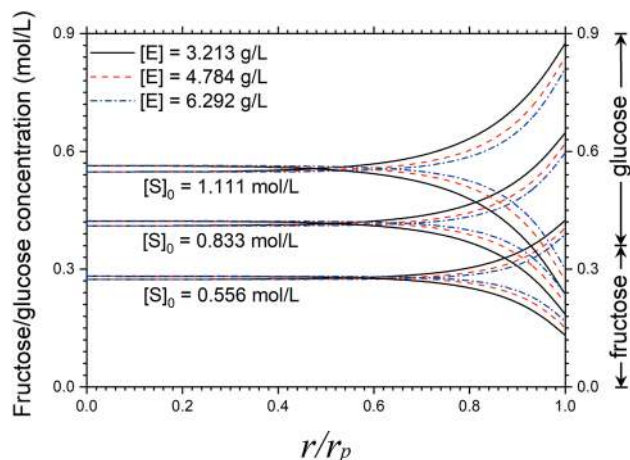
Regarding the numerical aspects in the resolution of the mathematical equations system, the independence of the mesh in the discretization of Equation (11) was ensured, and 25 finite elements were used for the results, obtaining a SSWR $= 3.253 \times 10^{-3}$ with $W_j = 1$: $j = 1$, D_{eff}; $j = 2$, η. On the other hand, the selection of OCM-HCS is due to the fact that this method provides precise approximations of the first derivative for the unknown function, and in this case, the radial component of the concentration gradient ($\partial c_i / \partial r$). This is required in the balance of chemical species obtained from the principle of matter conservation in the fluid phase (Equation (14)).

In addition, Figure 6 shows the intraparticle concentration profiles of glucose and fructose simulated in all of the experimentally studied treatments, $t = 210$ min, and it is observed that glucose conversion occurs in the radial region $0.5 \leq r/r_p \leq 1$ only; that is, up to 210 min, the intraparticle mass transfer resistance is still significant. In this sense, an improvement in the production of fructose establishes the need to reduce the size of the biocatalytic bead, which will allow any actively available enzyme to be used.

When examining the dynamics of the intraparticle glucose concentration profiles at different reaction times (Figure 7), the radial region where glucose conversion occurs is similar to that obtained at 210 min, i.e., $0.5 \leq r/r_p \leq 1$. It is important to mention that in irreversible reaction processes with immobilized enzyme, the effect of penetration in intraparticle mass transfer is accentuated more as the reaction develops over time, which contrasts with what was observed in this work since the reversible reaction causes a reduction in the penetration of the intraparticle mass transfer.

Simulation of Immobilized Enzyme Kinetics

In order to improve the IERS, it is essential to understand the effect of the bead synthesis process on the metabolite productivity.

particle to be in a completely stationary state. Baronas et al.[31] presented a mathematical model for an STR using immobilized enzyme. Three regions were involved in the model: (1) an array of porous microreactors (MRs) loaded with enzyme, where both the enzymatic reaction and mass transfer by diffusion occurs; (2) a diffusion limiting region surrounding the particles; and (3) a convective region where the substrate possessed uniform concentration. The MRs were modelled mathematically using a two-compartment model based on reaction-diffusion equations that contain a non-linear term related to the kinetics of Michaelis-Menten enzymes. Although the research of Baronas et al.[31] articulates similar ideas to those proposed in our research, it does

Figure 6. Profiles of intraparticle glucose and fructose concentration obtained from the bioconversion of glucose to fructose using CAB with a radius of 1.5 mm in a STR, at 210 min of reaction, 65 °C, and different substrate concentrations.

Among the main factors influenced by the immobilization process are porosity, EDC, FREA, particle size, and ratio of enzyme mass/biocatalytic bead mass, among others. Some of these factors are easy to manipulate (i.e., particle size), while others are not (i.e., FREA). The latter is the result of complex decisions in terms of the selection of precursor compounds and the synthesis process of catalytic beads, which could compromise other desirable attributes, such as its thermal and mechanical resistance. In this sense, it is very important to carry out, *a priori*, a theoretical evaluation in order to establish the impact of the aforementioned factors on productivity and, subsequently, to explore new materials and procedures that enable the improvement of the characteristics of the immobilizer matrix structure. In this way, Figure 8 shows the effects of FREA, particle size, EDC, and the volumetric fraction of biocatalytic beads on the kinetics of fructose production in an STR using immobilized enzyme. Figure 9 shows the intraparticle glucose concentration profiles achieved in the biocatalytic bead at 12 h for the performed simulations.
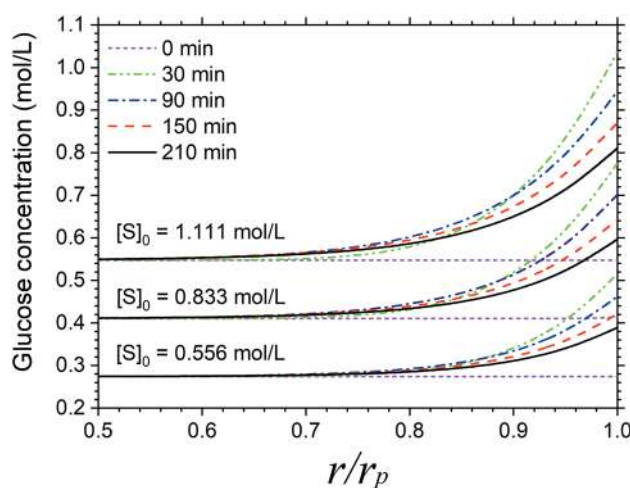

Figure 7. Profiles of intraparticle glucose concentration obtained from the bioconversion of glucose to fructose using CAB with a radius of 1.5 mm in a STR, at 0, 30, 90, 150, and 210 min of reaction, 65 °C, 6.292 g/L of immobilized enzyme, and different substrate concentrations.

In Figure 8a, it is observed that at each time step, the variation in fructose production is increased as the FREA increases. In fact, in Figure 9a, the variation in this factor has a pronounced effect on the radial depth at which the reaction rate is significant. This has such a significant effect that for an efficiency of 0.25, the diffusion mechanism is faster than the reaction mechanism, since in the centre of the particle the glucose concentration has displaced from equilibrium. Thus, for practical purposes, ensuring an efficiency that is greater than 0.5 could be adequate in order to achieve an acceptable amount of productivity. Note that the efficiency is affected by the immobilization conditions (mainly temperature and pH) as well as by the structure of the immobilization matrix, which can trap or obstruct the active sites of the enzyme. Therefore, establishing biocatalytic bead synthesis conditions that improve the value of this factor at the experimental level represents a real challenge, since the manipulation of the synthesis process could also significantly affect the mechanical and thermal resistance of the biocatalytic support. In general, it is expected that immobilization processes decrease the enzymatic catalytic activity. In addition, it is typical that the studies on the IERS are established in terms of apparent parameters, in which it is not possible to distinguish between the diffusion and reaction mechanism. This is done with the purpose of providing the necessary technical information for bioreactors design, but inevitably is restricted to the operation and bead synthesis conditions considered under study.

Concerning the selection of the CAB radius, Figure 8b shows the effect of this factor (ranging from 0.5−2.5 mm) on the kinetics of fructose production, which is accentuated because at a lower bead radius, the contact area to bead volume ratio is increased. Therefore, according to Figure 9b, the relative radial region where glucose to fructose conversion occurs ($0.6 \leq r/r_p \leq 1$) is similar for almost all of the studied particle sizes (except for $r_p = 0.5$ mm because the equilibrium condition had already been reached). The kinetic mechanism could be considered as a surface reaction instead of a volumetric reaction, which is a result of the high resistance of the diffusive mass transfer in the biocatalytic bead. Thus, the use of CABs with a radius of 0.5 mm is recommended since this allows higher bioconversions at low operating times to be obtained; besides, the manipulation of the bead size is relatively easy to obtain experimentally. With respect to the EDC obtained for the biocatalytic beads, it was found to be approximately 80 times smaller than that for glucose in an aqueous solution (7×10^{-10} m²/s),[28] which could be considered a significant difference because the main component of the beads is water with a composition higher than 90 %. Therefore, it can be inferred that the polymeric matrix of calcium alginate significantly restricts the mobility of water molecules, causing the diffusion capacity of a solute to be significantly diminished. Figure 8c shows the effect that the EDC has on the fructose production, and it is observed that when the resistance of the intraparticle mass transfer is high, the reaction system behaves like pseudo-zero order kinetics because only the surface region of the biocatalytic bead participates in the bioconversion (Figure 9c), and this increases the time scale of the process. In contrast, with a higher EDC, even under a value close to the diffusion coefficient in aqueous solution (1×10^{-10} m²/s), the characteristic time required for the maximum bioconversion is 6 h, which contrasts with the time required for the EDC obtained by adjusting the experimental data (higher than 12 h). In this sense, the experimental manipulation required to improve the EDC of the immobilization matrix is not as significant as the
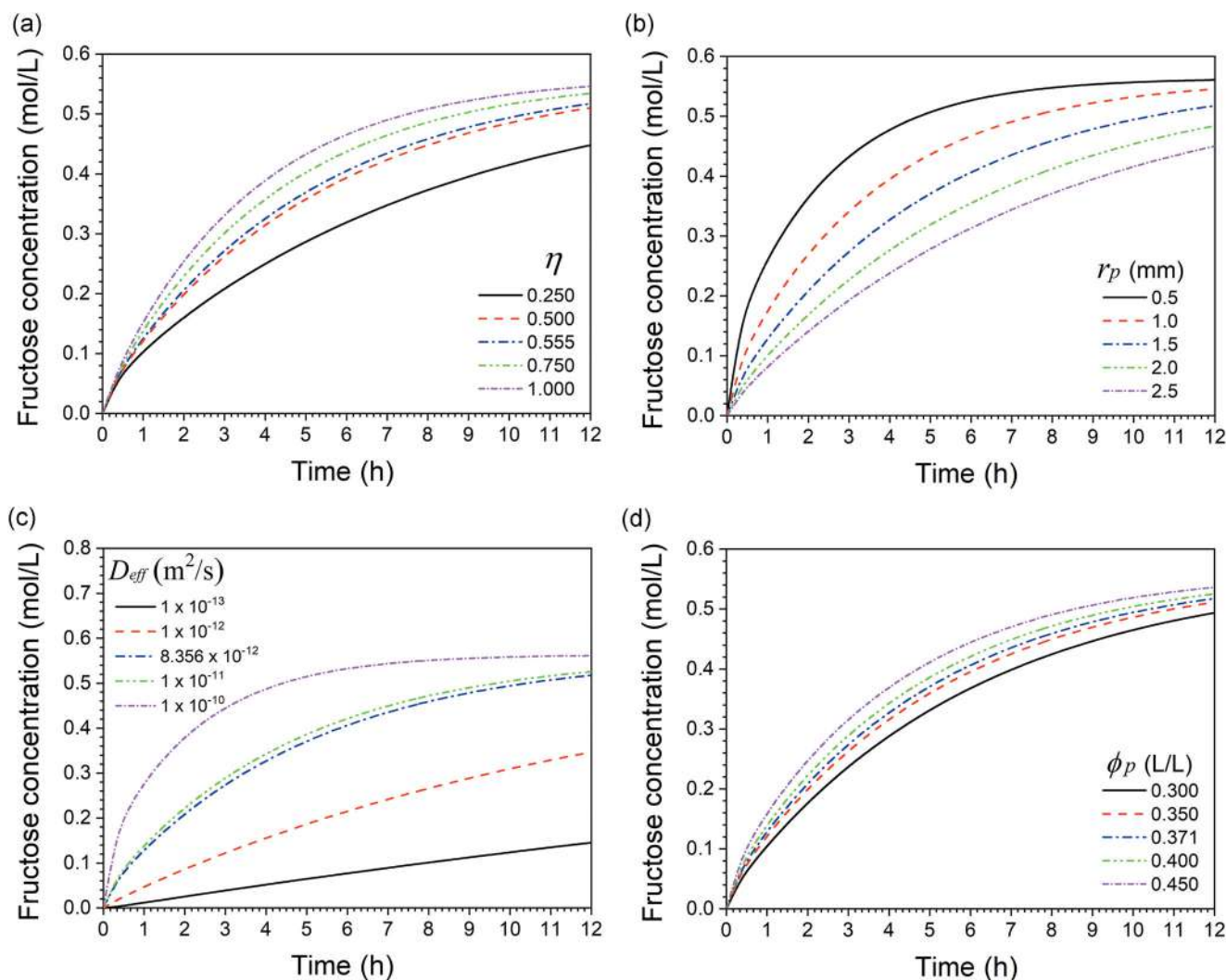
Figure 8. Effect of: (a) FREA, (b) radius of the biocatalytic bead, (c) EDC, and (d) volumetric fraction of biocatalytic beads on the history of fructose concentration in the fluid phase, resulting from the glucose to fructose bioconversion in a STR at 65 °C, 6.292 g/L of immobilized enzyme in CAB, and 1.111 mol/L of glucose.
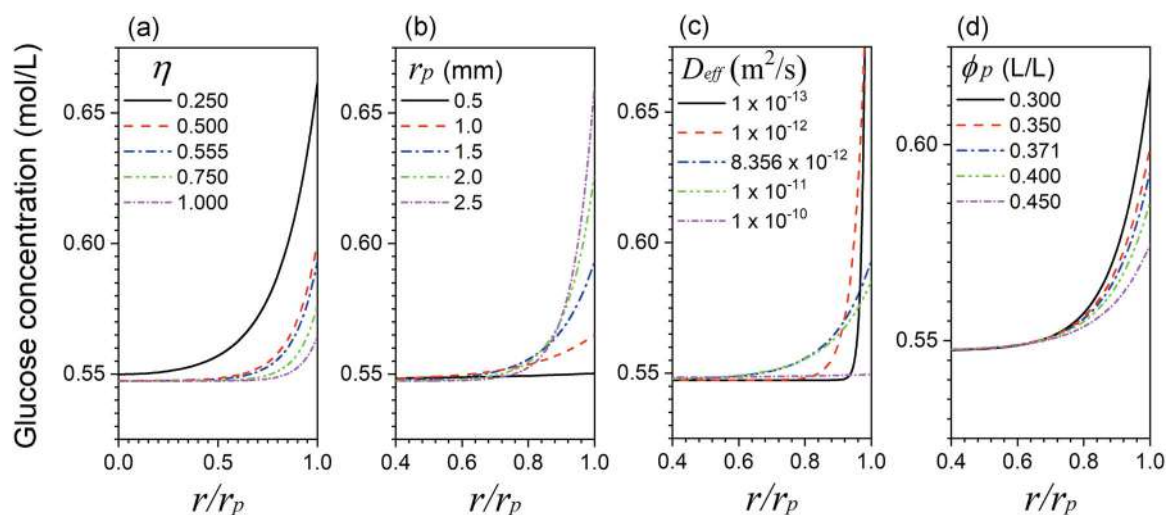
Figure 9. Effect of: (a) FREA, (b) radius of the biocatalytic bead, (c) EDC, and (d) volumetric fraction of biocatalytic beads on the profiles of intraparticle glucose concentration, resulting from the glucose to fructose bioconversion in a STR at 65 °C, 12 h, 6.292 g/L of immobilized enzyme in CAB, and 1.111 mol/L of glucose.

improvement provided by the reduction in the bead size; With $r_p = 0.5$ mm, a similar kinetic behaviour to that obtained with $D_{eff} = 1 \times 10^{-10}$ m²/s is achieved. Finally, the effect of the bead volumetric fraction on the productivity is analyzed, which, under a constant ratio of $m_{E,t}/V_t$, can be interpreted as the effect of the enzyme concentration inside the bead. Thus, according to the selected range (0.30−0.45 L/L), it can be seen in Figure 8d that it was the least significant effect on productivity, with a very similar behaviour among the different simulated kinetics. This is due to the fact that the resistance of the bead to the diffusive mass transfer regulates the bioconversion process through the effective volumetric reaction region, which is similar in all cases for the volumetric fraction of the selected beads (Figure 9d). Interestingly, it is observed that a high volumetric fraction of beads (low enzyme concentrations inside the bead) promotes the best productivity. This is because the reaction mechanism in the bead behaves as a surface reaction. Therefore, the increase in the fluid-solid contact surface (which occurs when the volumetric fraction of beads is high) is more important than the increase in the enzyme concentration in the bead. In fact, the depth at which the bioconversion occurs in the bead is essentially the same for the different volumetric fractions of beads. Therefore, the glucose flux is regulated by the glucose concentration in the fluid phase, which, in this case, is higher for low volumetric fractions of beads since the bioconversion rate is slower as it is further away from equilibrium conditions.

CONCLUSIONS

A new approach was presented for the analysis of kinetic and diffusional effects of an immobilized enzyme reaction system. A mathematical model was established in which the concept of the fraction of residual enzymatic activity (FREA) was incorporated. The volumetric reaction rate within a biocatalytic bead was described mathematically in terms of enzyme concentration, similar to what occurs in free enzyme processes, i.e., through the ratio of total enzyme mass/total bioreaction volume. Therefore, it was feasible to separately determine both the diffusional effects (effective diffusivity coefficient, EDC) and the kinetic effects (FREA). In order to achieve this, the experimental results of the glucose/fructose bioconversion kinetics using free and immobilized glucose isomerase were presented. In the case of free enzyme experiments, the effects of the type of substrate (glucose or fructose), substrate concentration, temperature, and enzyme concentration on the product formation were evaluated and a set of experimental data was generated and used in the simultaneous adjustment of the Arrhenius parameters in relation to the Briggs-Haldane reversible mechanism. The following numerical strategy was established: first, a linearized algebraic form with respect to the Michaelis-Menten kinetic parameters was obtained for the direct/reverse reaction (V_{mf}, K_{mf}, V_{mr}, and K_{mr}); and, subsequently, the Arrhenius parameters (A_m and $E_{a,m}$) were adjusted by applying the Gauss-Newton method, since the kinetic model is not linear with respect to temperature. As a result, a strategy was found to determine the numerical solution in which explicit descriptions of the Jacobian and Hessian were used. On the other hand, in the case of experiments with immobilized enzyme, the effects of substrate and enzyme concentration on the fructose production was studied, in which the generated experimental data enabled the evaluation of the EDC and the FREA. Therefore, it was possible to establish a mathematical model in which the kinetic and diffusional mechanisms of the biocatalytic bead are described from the kinetic parameters obtained in free enzyme

reaction systems (FERS). Furthermore, the partial differential equation associated with the substrate/product intraparticle concentrations was discretized by the orthogonal collocation method using Hermite cubic splines, guaranteeing precise numerical solutions, even in the case of high concentration gradients, which occurs at low effective diffusion coefficients. Thus, through simulation it was possible to analyze the effects of FREA, bead size, EDC, and the volumetric fraction of the biocatalytic beads on the kinetics of fructose production, which made it possible to understand that the FREA evaluated by experimental kinetics is adequate. In addition, it was determined that the bead size (which should be decreased) is the easiest factor to manipulate and that it has a favourable effect on fructose production. In general, both the numerical strategies and the conceptual model of the biocatalytic bead established in this work significantly facilitate the analysis of kinetic and diffusional effects, and the results could potentially serve as a guide in the improvement of the synthesis processes of biocatalytic beads.

NOMENCLATURE

A	pre-exponential factor (g/(mol · s))
a, b	square root of the Arrhenius parameters
$\hat{a}_p$	specific particle area (1/m)
B_1, B_{21}, B_{22}	parameters used in Equation (16)
c_1	substrate concentration (mol/L)
c_2	product concentration (mol/L)
C_i	liquid phase concentration (mol/L)
D_{eff}	effective diffusivity coefficient (m²/s)
D_{st}	stirrer diameter (m)
D_{ir}	internal reactor diameter (m)
E	enzyme
$[E]$	enzyme concentration (g/L)
$[E]_{imm}$	immobilized enzyme concentration (g/L)
E_a	activation Energy (J/mol)
$H_{r_i,\vec{p}}$	Hessian of r_i with respect to the $\vec{p}$ adjustment parameters
h_L	fluid height (m)
$J_{\vec{r},\vec{p}}$	Jacobian of residual vector $\vec{r}$ with respect to the adjustment parameters $\vec{p}$
k_1, k_{-2}	intermediary reaction rate constants, (g/(mol · s))
k_2, k_{-1}	intermediary reaction rate constants (mol/(g · s))
K_{eq}	equilibrium constant
k_L	convective mass transfer coefficient in the fluid phase (m/s)
K_m	Michaelis-Menten affinity constant (mol/L)
K_{mf}	glucose to fructose Michaelis-Menten affinity constant (mol/L)
K_{mr}	fructose to glucose Michaelis-Menten affinity constant (mol/L)
m_E	enzyme mass (g)
P	product
r	radius (m)
$-\mathbf{r}_1$	substrate consumption reaction rate (mol/(L · s))
$\mathbf{r}_2$	product generation reaction rate (mol/(L · s))
$\mathbf{r}_i$	free enzyme reaction rate (mol/(L · s))

$\hat{r}_i$	volumetric reaction rate (mol/(L · s))
r_p	biocatalytic bead radius (m)
$\vec{r}(\vec{p}_n)$	vector of residuals as function of the adjustment parameters vector
S	substrate
SSE	sum of the squared errors
SSWR	sum of the squares of the weighed residuals
t	time (s)
V_t	total reaction volume (L)
V_p	total beads volume (L)
V_∞	supernatant volume (L)
V_m	maximum reaction rate (mol/(L · s))
V_{mf}	glucose to fructose maximum reaction rate (mol/(L · s))
V_{mr}	fructose to glucose maximum reaction rate (mol/(L · s))
$\bar{V}_{mf}$	glucose to fructose maximum specific reaction rate (mol/(g · s))
$\bar{V}_{mr}$	fructose to glucose maximum specific reaction rate complex
$\Delta c_{2,m}$	logarithmic mean of the differences in final and initial concentrations (mol/L)

Greek Letters

α, β, γ	parameters used in Equation (19)
ε	porosity (L/L)
η	fraction of residual enzymatic activity
θ	unaccomplished product ratio
φ	volumetric fraction of liquid-phase in bioreactor (L/L)
ω	sub-relaxation factor (Equation (23))

Subscripts

eq	equilibrium (Equation (15))
exp	experimental conditions
i	chemical species (glucose = 1, fructose = 2)
m	elementary reaction rate (Equation (5))
t	total
0	initial condition (Equation (7))

REFERENCES

[1] W. Aehle, *Enzymes in Industry: Production and Applications*, 2nd edition, Wiley-VCH, Weinheim **2007**.

[2] C. Simionescu, S. Dumitriu, M. Popa, M. Dumitriu, D. Hritcu, *Colloid Polym. Sci.* **1984**, *262*, 705.

[3] A. Kilara, K. M. Shahani, T. P. Shukla, *Crit. Rev. Food Sci.* **1979**, *12*, 161.

[4] K. Won, S. Kim, K. J. Kim, H. W. Park, S. J. Moon, *Process Biochem.* **2005**, *40*, 2149.

[5] A. A. Homaei, R. Sariri, F. Vianello, R. Stevanato, *Journal of Chemical Biology* **2013**, *6*, 185.

[6] T. M. Abdel-Rassol, S. A. Badr, H. T. Omran, *Afr. J. Biotechnol.* **2012**, *11*, 15798.

[7] S. H. Bhosale, M. B. Rao, V. V. Deshpande, *Microbiol. Rev.* **1996**, *60*, 280.

[8] L. Zittan, P. Poulsen, S. H. Hemmingsen, *Starch-Stärke* **1975**, *27*, 236.

[9] A. Martinsen, G. Skjåk-Bræk, O. Smidsrød, *Biotechnol. Bioeng.* **1989**, *33*, 79.

[10] H. Tumturk, G. Demirel, H. Altinok, S. Aksoy, N. Hasirci, *J. Food Biochem.* **2008**, *32*, 234.

[11] F. Camacho-Rubio, E. Jurado-Alameda, P. González-Tello, G. Luzón-González, *Can. J. Chem. Eng.* **1995**, *73*, 935.

[12] A. Converti, M. Del Borghi, *Bioprocess Eng.* **1997**, *18*, 27.

[13] V. Bravo, E. Jurado, G. Luzón, N. Cruz, *Can. J. Chem. Eng.* **1998**, *76*, 778.

[14] S. S. Tükel, D. Alagöz, *Food Chem.* **2008**, *111*, 658.

[15] H. Zhao, Q. Cui, V. Shah, J. Xu, T. Wang, *J. Mol. Catal. B-Enzym.* **2016**, *126*, 18.

[16] D. X. Jia, T. Wang, Z. J. Liu, L. Q. Jin, J. J. Li, C. J. Liao, D. S. Chen, Y. G. Zheng, *J. Biosci. Bioeng.* **2018**, *126*, 276.

[17] A. R. Özdural, D. Tanyolaç, Z. Demircan, I. H. Boyaci, M. Mutlu, C. Webb, *Chem. Eng. Sci.* **2001**, *56*, 3483.

[18] T. M. Silva, A. R. de Lima Damásio, A. Maller, M. Michelin, F. M. Squina, J. A. Jorge, M. D. L. T. De Moraes, *Folia Microbiol.* **2013**, *58*, 495.

[19] A. Das, T. Paul, P. Ghosh, S. K. Halder, P. K. D. Mohapatra, B. R. Pati, K. C. Mondal, *Waste Biomass Valori.* **2015**, *6*, 53.

[20] J. Rakmai, B. Cheirsilp, *Biochem. Eng. J.* **2016**, *105*, 107.

[21] J. R. Dormand, P. J. Prince, *J. Comput. Appl. Math.* **1980**, *6*, 19.

[22] J. C. Lagarias, J. A. Reeds, M. H. Wright, P. E. Wright, *SIAM J. Optimiz.* **1998**, *9*, 112.

[23] E. Palazzi, A. Converti, *Biotechnol. Bioeng.* **1999**, *63*, 273.

[24] A. M. Dehkordi, M. S. Tehrany, I. Safari, *Ind. Eng. Chem. Res.* **2009**, *48*, 3271.

[25] R. Giordano, R. Giordano, C. Cooney, *Bioprocess Eng.* **2000**, *23*, 159.

[26] E. Palazzi, A. Converti, *Enzyme Microb. Tech.* **2001**, *28*, 246.

[27] I. L. Andresen, O. Smidsørod, *Carbohyd. Res.* **1977**, *58*, 271.

[28] A. Axelsson, B. Persson, *Appl. Biochem. Biotech.* **1988**, *18*, 231.

[29] P. Grunwald, *Biochem. Educ.* **1989**, *17*, 99.

[30] C. M. Bidabehere, J. R. García, U. Sedran, *Chem. Eng. J.* **2018**, *345*, 196.

[31] R. Baronas, J. Kulys, L. Petkevičius, *J. Math. Chem.* **2018**, *57*, 327.